

An Integrated AC Drive System Using a Controlled-Current PWM Rectifier/Inverter Link

BOON TECK OOI, SENIOR MEMBER, IEEE, JUAN W. DIXON, ASHOK B. KULKARNI,
AND MASAHIRO NISHIMOTO

Abstract—Two identical 3-phase, bipolar transistor, controlled-current, pulsewidth modulation power modulators are integrated so that one functions as a rectifier and the other as an inverter in an ac drive system. The rectifier input currents maintain near 60-Hz sinusoidal waveforms with unity factor. Leading power factor option is available. The modulators do not depend on the availability of bidirectional switch elements. Performance as a polyphase induction motor drive under motoring and regenerative braking is reported. The study includes digital simulation of operation as a synchronous motor drive.

INTRODUCTION

THE pulsewidth modulation (PWM) converter is a potential challenge to the venerable thyristor Graetz bridge at the rectifier end of the variable-speed ac drive system. The merits of the current-controlled PWM power modulator are:

- 1) it delivers near-sinusoidal currents, thus obviating expensive low-harmonic filters;
- 2) it is capable of unity and even leading power factor operation, thus offering the option of power factor compensation;
- 3) it has bidirectional power flow capability as compared to the need of dual converters of the Graetz bridge configuration.

As is apparent in the sparse literature [1]–[6], the application of the PWM modulator as a rectifier is still in the fledgling state of its development. However, once its claims to superior performance become more fully established, utilities will become less tolerant of the harmonic pollutions from the thyristor Graetz bridges and one can expect stricter harmonic legislation.

The objective of this paper is to report on the successful integration of two identical experimental current-controlled PWM power modulators to form the rectifier/inverter pair in the frequency changer for variable-speed ac drive systems.

Manuscript received July 8, 1986; revised July 14, 1987. This work was supported by the Natural Science and Engineering Research Council of Canada and the Ministry of Education, Province of Quebec, through an FCAR grant. This paper was presented at the IEEE Power Electronics Specialists Conference, Vancouver, BC, Canada, June 23–27, 1986.

B. T. Ooi, J. W. Dixon, and M. Nishimoto are with the Department of Electrical Engineering, McGill University, 3480 University St., Montreal, PQ, H3A 2A7 Canada.

A. B. Kulkarni is at Texas A&M University, College Station, Texas 77843, USA.

IEEE Log Number 8717896.

Research along this line has been pioneered in [7]–[9]. The PWM modulators in this paper do not depend on the availability of bidirectional switches. Instead each switch element consists merely of a bipolar transistor (or GTO or power FET) with a freewheeling diode connected in parallel. Under the inverter mode of operation, the current flows preponderantly through the transistor. Under the rectification mode of operation, the current path is preponderantly through the freewheeling diode, which is made conducting by the $L di/dt$ voltage across the inductance on the ac side of the circuit.

CONTROLLED CURRENT PWM CONVERTER/INVERTER LINK

The plan of the integrated variable-speed drive system is shown in Fig. 1.

The Load

The ac motor is driven by a current-controlled PWM inverter. The motor control can be very sophisticated and may include speed and current feedback with field vector strategies. However, such complication is beyond the scope of this study. The objective here is merely to test the practicability of the rectifier/inverter link and to allow any inherent problems to surface to one's attention. In this study, the frequency control ω_i and the current magnitude control I_{mag} are left as open-loop controllers.

Basic to the operation of the current-controlled PWM inverter is the generation of the reference waveforms:

$$u_R = \sin \omega_i t \quad (0-a)$$

$$u_s = \sin (\omega_i t - 120^\circ) \quad (0-b)$$

$$u_T = -u_R - u_s. \quad (0-c)$$

These are multiplied by the current magnitude control I_{mag} to form the template waveforms:

$$i_R = I_{mag} u_R \quad (0-d)$$

$$i_s = I_{mag} u_s \quad (0-e)$$

$$i_T = I_{mag} u_T. \quad (0-f)$$

The output phase currents i_R , i_s , and i_T of the inverter are measured through Hall-effect transducers and are made to track the template waveforms by applying the ON-OFF switchings of the bipolar transistors in a negative feed-

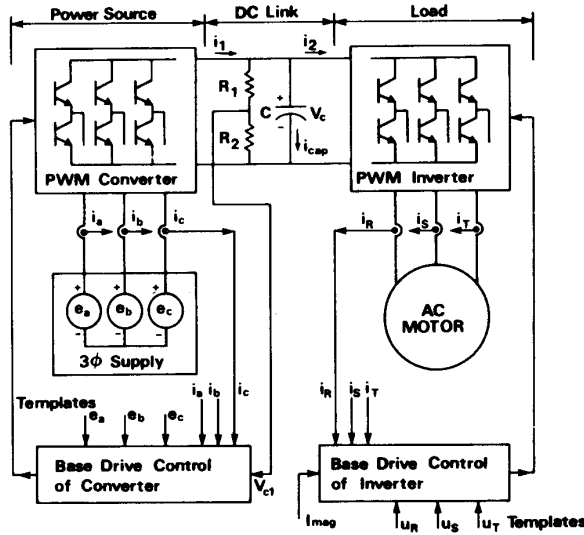


Fig. 1. Schematic of controlled-current PWM rectifier/inverter ac drive.

back mode. The hysteresis control which accomplishes this is represented by the block: Base Drive Control.

The AC Power Source

On the power source side is an identical controlled-current PWM modulator which is normally operated as a rectifier. The ac terminals of the modulators are connected to the 60-Hz three-phase source voltages e_a , e_b , and e_c .

The reference waveforms are taken through voltage transformers from the phase voltages of the 60-Hz sources. Phase shifting is introduced for power factor correction. Some electronic filtering is found necessary to remove the third harmonic introduced by transformer saturation. Current magnitude control is introduced by multiplying the reference waveforms by I_m to form the current templates. As in the inverter, the phase currents are made to track the template waveforms within a narrow tolerance band of width h by a hysteresis control in the Base Drive Control.

DC Link

The two PWM modulators are connected at the dc link. The shunt capacitor C serves two functions: 1) that of a ripple filter, and 2) that of a charge storage to maintain a sizeable dc link voltage V_c .

OPERATING CHARACTERISTICS OF CURRENT-CONTROLLED PWM MODULATORS

The integration of two PWM modulators to form the rectifier/inverter link must consider the idiosyncrasy of the individual modulator. As its name suggests, the significant peculiarity comes from the fact that the phase currents of the modulator are controlled by the template waveforms. The first design considerations which must be observed are the limits within which the phase currents are capable of tracking the template waveforms. Previous work [6] has identified that there are two limits, which

have been given the names *loss of control limit* and *current waveform distortion limit*.

The second design consideration is one of ensuring that the current control of the inverter and the current control of the rectifier be coordinated so that the power demanded by the ac motor is matched by the power supplied by the 60-Hz ac voltage sources. The command which signals a reversal of power flow in the inverter must also simultaneously signal a reversal in the rectifier.

Loss of Control Limit

The loss of control limit is relevant in the rectifier regime of operation only. A cursory glance over Fig. 2 will call attention to the fact that the 6 freewheeling diodes across the transistors $T1, T2, \dots, T6$ form a diode bridge which can rectify power from ac voltage sources e_a, e_b , and e_c . A *sine qua non* of the PWM rectifier operation is that the voltage V_c across the dc link is always high enough so as to reverse-bias all these diodes. Normal PWM rectifier operation consists of initially building up magnetic storage energy in the inductance L by "shorting" the phase voltage through an ON-transistor for a brief instant, then turning OFF the transistor and allowing the $L di/dt$ voltage to force the storage magnetic energy through the freewheeling diode to the dc link. In [6] it was estimated that the PWM rectifier loses control when

$$V_c < \sqrt{6} |\tilde{V}_m| 3/\pi \quad (1)$$

where $|\tilde{V}_m|$ is the rms phase ac voltage measured at the modulator terminals.

Because of the loss of control limit, a special initiation procedure is required in "starting the rectifier/inverter system from the cold." This procedure will be described in a later section. It consists of ensuring that the dc link capacitor is charged to a voltage above the loss of control limit prior to switching on the ac supply.

Current Distortion Limit

When the ac phase voltage at the modulator terminals \tilde{V}_m has a magnitude which exceeds the dc link voltage V_c in the inequality

$$V_c < \sqrt{6} |\tilde{V}_m|, \quad (2)$$

there is insufficient resultant voltage to force the currents through the inductances so as to track the desired template waveforms. Equation (2) has been derived analytically, although no proofs have been published. Reference [6] has given experimental results which substantiated the correctness of (2).

Power Matching in Modulators

Using the symbols $\tilde{V}_m, \tilde{I}, \phi$ to denote the rms value of the phase voltage at the ac terminals of the modulator, the phase current, and the power angle, respectively, and furthermore using the subscripts r and i to denote quantities in the rectifier and the inverter side, the static power continuity of the dc link (neglecting modulator losses) is

$$3 |\tilde{V}_{mr}| |\tilde{I}_r| \cos \phi_r = 3 |\tilde{V}_{mi}| |\tilde{I}_i| \cos \phi_i. \quad (3)$$

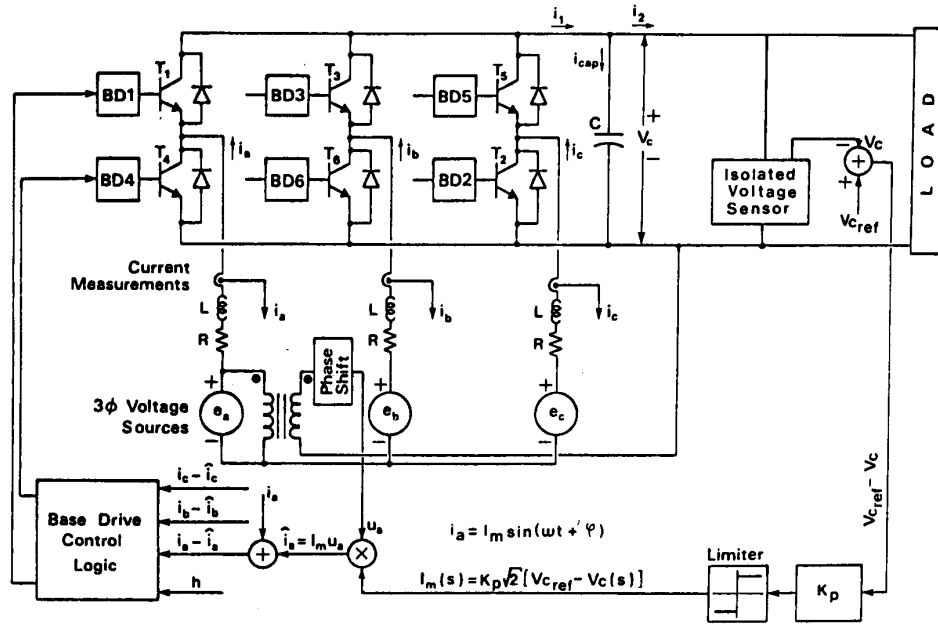


Fig. 2. Schematic of rectifier controls. Proportional feedback to achieve regulated dc link voltage.

On the rectifier side, ϕ_r is set by the phase-shift control. When the rectifier ac side resistances and inductances are small, V_{mr} is approximately the voltage of the ac supply. The controllable element is $|\tilde{I}_r|$, which is controlled by I_m in Fig. 1 where

$$|\tilde{I}_r| = \frac{I_m}{\sqrt{2}} \quad (4)$$

On the inverter side, the phase current magnitude $|\tilde{I}_i|$ is controlled by I_{mag} in Fig. 1:

$$|\tilde{I}_i| = \frac{I_{mag}}{\sqrt{2}} \quad (5)$$

However, both $|\tilde{V}_{mi}|$ and ϕ_i depend on the type of motor connected to the inverter as well as its operating speed and torque. One can conceive of complicated real-time controls where the motor speed and currents are measured, \tilde{V}_{mi} and ϕ_i estimated from the equations of the plant, and \tilde{I}_r calculated from (3) and applied as a feed-forward command to the rectifier control I_m in (4). However, such sophistication will be deferred to later studies if the simpler control described here proves to be inadequate.

REGULATED DC LINK VOLTAGE CONTROL

The three above-mentioned constraints are simultaneously respected by applying a simple proportional feedback control around the rectifier as shown in Fig. 2. This control ensures that the voltage V_c across the dc link is regulated at a level well above both the loss of control limit and the current waveform distortion limit. The voltage is maintained by the electric charge deposited in the filter capacitor, C . The idea consists of controlling the rectifier output i_1 to replenish the charge drained by the

inverter current i_2 . Thus in maintaining a constant voltage across the dc link one ensures that the power demand is always matched by the power supply.

Rectifier Side

Fig. 2 consists of a more detailed plan of the PWM converter of Fig. 1. The three-phase ac supplies are represented by e_a , e_b , and e_c . As illustrated by the a phase, the template waveform is taken from the potential transformer, phase shifted, and then multiplied by the magnitude control I_m .

Neglecting losses in the transistors and the diodes, the balance of dc and ac power on the rectifier side is

$$V_c i_1 = 3 |\tilde{V}_{mr}| |\tilde{I}_r| \cos \phi_r \quad (6)$$

On substituting (4) into (6),

$$i_1 = \frac{3 |\tilde{V}_{mr}| I_m \cos \phi_r}{\sqrt{2} V_c} \quad (7)$$

Inverter-Motor Side

The inverter-motor side is represented by the block labelled "load" in Fig. 2. Based on the balance of dc power and ac power on the inverter side, one has

$$v_c i_2 = 3 |\tilde{V}_{mi}| |\tilde{I}_i| \cos \phi_i \quad (8)$$

and

$$i_2 = \frac{3 |\tilde{V}_{mi}| I_{mag} \cos \phi_i}{\sqrt{2} V_c} \quad (9)$$

Capacitor Voltage Control

From (6) and (8), one sees that the ac power matching problem is solved when the dc power is matched in the dc

link; that is

$$V_c(i_1 - i_2) = 0. \quad (10)$$

One notes that the filter capacitance voltage is

$$V_c(t) = \frac{1}{C} \int_{-\infty}^t i_{CAP} dt' \quad (11)$$

$$\begin{aligned} &= \frac{1}{C} \int_{-\infty}^0 [i_1(t') - i_2(t')] dt' \\ &+ \frac{1}{C} \int_0^t [i_1(t') - i_2(t')] dt'. \end{aligned} \quad (12)$$

If one ensures that in (12),

$$\frac{1}{C} \int_0^t [i_1(t') - i_2(t')] dt' = 0 \quad (13)$$

for $t \geq 0$, then

$$\begin{aligned} V_c(t) &= \frac{1}{C} \int_{-\infty}^0 [i_1(t') - i_2(t')] dt' \\ &= \text{constant} \end{aligned} \quad (14)$$

for $t > 0$.

Clearly, when (10) is satisfied, (13) is also satisfied. The constant voltage in (14) is the voltage to which the capacitor is charged prior to $t = 0$, and this voltage must be chosen well above the loss of control limit and the current waveform distortion limit.

Regulated Voltage Feedback

From the previous discussion, one sees that one merely needs to apply the lever of control I_m of the rectifier in a feedback loop to maintain a regulated voltage across the dc link. This sets the inverter side levers I_{mag} and ω_i free for the motor control.

As shown in Fig. 2, the implementation of the regulated voltage feedback starts from a dc power supply from which a reference voltage V_{CREF} is set. The capacitor V_c is measured and compared with the reference. The error after passing through a transfer function $G(s)$ and a current limiter is used as the magnitude control I_m . From (7) one sees that i_1 is called upon by I_m to null the error.

The transfer function $G(s)$ offers the option of combinations of proportional, integral, and differential control. As an initial study, it was decided to implement a proportional control. One can return to the more complicated transfer functions should the performance of the proportional control prove to be poor.

In the proportional control, there is a voltage droop as a function of dc load current. This droop has not been found to be a serious defect in the overall performance.

LABORATORY MODEL

The photo in Fig. 3 shows the hardware implementation. Each modulator consists of three switch modules. Each module is comprised of the upper and the lower bipolar transistor/diode switch units of one phase. In Fig.

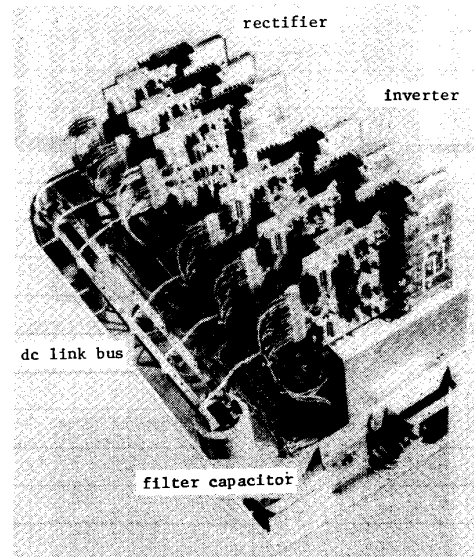


Fig. 3. Photo showing rectifier/inverter units. Each unit consists of three switch modules. DC link buses shown on left with filter capacitors across them.

3, one sees the rectifier and the inverter connected to the dc link buses which have the filter capacitors across them.

Because of budgetary constraints, the ratings are modest. The open circuit dc link voltage is set at $V_{co} = 110$ V and the current limit at 5 A dc.

INITIATION CIRCUIT AND INITIATION PROCEDURE

When starting from "cold," the dc link filter capacitor C is initially discharged. An initiation circuit is used together with an initiation procedure to charge the filter capacitor well above the loss of control limit and the current waveform distortion limit before the activation of the rectifier, and thereafter, the activation of the inverter.

The initiation circuit consists simply of a diode rectifier supplied by a voltage transformer. As its function is merely to charge the filter capacitor, its current rating need only be very low. A series resistance is introduced to limit the inrush current. The voltage output of the initiation circuit is chosen *above* the two aforementioned limits but *below* the operating range determined by the reference voltage V_{CREF} of the voltage regulator feedback. After the rectifier has been activated, the voltage error of the feedback loop causes i_1 to continue charging the filter capacitor to the open circuit voltage V_{co} . As the voltage output of the initiation circuit is below V_{co} , its diodes become reverse-biased and the initiation circuit is effectively deactivated so that no charging current from it interferes with the accuracy of the regulator loop.

On switching the three ac voltages across rectifier terminals, the usual large inrush currents through the freewheeling diodes are prevented because the initiation circuit has already charged up the capacitor and back-biased the freewheeling diodes.

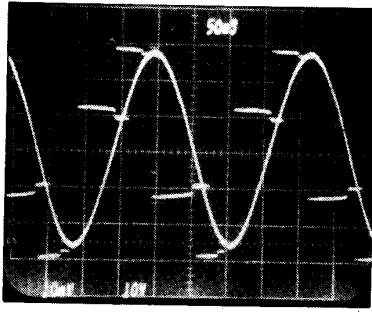


Fig. 4. Induction motoring mode. Near sinusoidal motor current lags voltage.

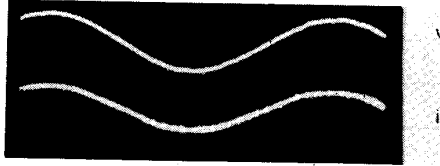


Fig. 5. Phase voltage and current on rectifier side under induction motoring condition.

TEST WITH POLYPHASE INDUCTION MOTOR

The rectifier/inverter system was connected to run a small polyphase induction motor. The motor was operated under open loop conditions. The leverages of control of the motor were: the frequency ω_i (from a variable frequency source) and the current magnitude I_{mag} .

Fig. 4 shows a typical oscillogram of the phase current and the phase voltage of the motor. The current lags the voltage as it is in the motoring mode of operation.

Fig. 5 shows the oscillogram of the phase current and the phase voltage on the ac side of the rectifier under motoring conditions. One sees that the power factor is unity and the current waveform is near sinusoidal. Under induction generation conditions, the current takes on the opposite polarity with respect to the voltage waveform.

Figs. 6 and 7 show the oscillograms of the dc-link current i_1 of the rectifier during motoring and induction generation, respectively. One sees that bidirectional power flow is achieved by bidirectional current flow.

Fig. 8 shows the transients during a reversal from motoring to regenerative braking. The motor was originally running at high frequency under steady-state condition. The frequency control was lowered abruptly by hand. Because of the heavy inertia of the rotor the mechanical speed did not change as fast as the electrical variables. Since the rotating magnetic flux speed became lower than the rotor speed, the machine entered the generation regime. Since both the modulators were delivering power, the voltage of the filter capacitor charged up above reference voltage.

Fig. 8(a) shows the rise of the dc link voltage V_c during the transient period. The positive error caused the modulator on the left-hand side to change from being a rectifier to an inverter.

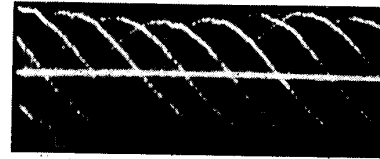


Fig. 6. Rectifier dc link current i_1 during induction motoring condition.



Fig. 7. Rectifier dc link current i_1 during induction generation condition.

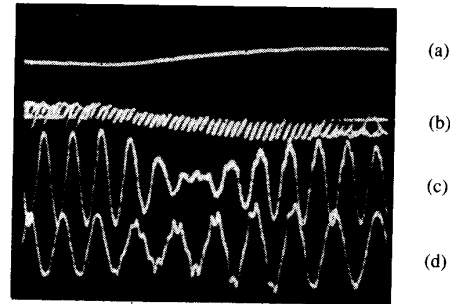


Fig. 8. Induction motor transition from motoring to regenerative braking. (a) DC link voltage V_c . (b) Rectifier side dc link current i_1 . (c) Rectifier side ac phase current. (d) Inverter side ac phase current.

Fig. 8(b) shows the rectifier dc link current, i_1 . The reversal of the direction of flow of the dc link current during the changeover from rectification to inversion is clearly evident.

The measured 60-Hz phase current on the ac supply side is displayed in Fig. 8(c). The transition from rectification to inversion appears as a 180° phase reversal of the current with respect to the ac supply phase voltage. The changeover occurs in the flattened portion of the oscillogram.

Fig. 8(d) displays the measured phase current of a motor phase. From the waveform, one sees the decrease of the frequency as the frequency control was turned by hand. One observes that the waveform distortion limit has been exceeded. This is because around zero slip, large controlled-current was being forced through the large magnetization reactance so that the ac phase voltage at the modulator terminals exceeded the limit set by (2).

STEP POWER REVERSAL TEST

The speed of response of the proportional feedback control of the rectifier in Fig. 8 was masked by two factors: a) the slow hand control in lowering the frequency reference, and b) the changing rotor speed. To remove these extraneous factors, the rectifier side was tested in isolation.

Initially, the rectifier side was operated as an inverter by injecting a dc current from an external current source at the dc link. A step power reversal was introduced by

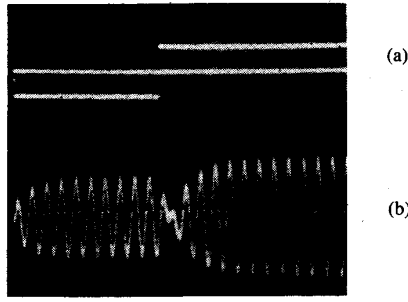


Fig. 9. Voltage regulated PWM modulator response to power reversal. (a) Step output current i_2 . (b) AC phase current showing 180° phase shift during reversal from inverter to rectifier mode of operation.

switching a resistance across the dc link. This resistance was chosen so that it drew a larger current than was provided by the external current source. This discharged the dc link capacitor and consequently the dc link voltage dropped so that the negative error commanded the change from inverter back to the normal rectifier mode of operation. Fig. 9(a) shows the output current i_2 undergoing the step change. Fig. 9(b) shows the ac phase current during the reversal from inverter to rectifier mode of operation. The transient was completed within four cycles of the 60-Hz supply.

DIGITAL SIMULATION OF SYNCHRONOUS MOTOR DRIVE Inverter-Synchronous Motor

It is assumed that the synchronous motor is equipped with a rotor position encoder, an erasable programmable read-only memory (EPROM) and a digital-analog converter (see [10]), by which the reference signals of (0-a, b, c) are generated in the form

$$u_R = \sin(\theta_i + \phi_i) \quad (15a)$$

$$u_S = \sin(\theta_i - 120^\circ + \phi_i) \quad (15b)$$

$$u_T = \sin(\theta_i - 240^\circ + \phi_i). \quad (15c)$$

Here θ_i is the rotor position and ϕ_i is its space phase angle referred to a stationary frame. As the rotor turns at ω_i electrical rad/s,

$$\theta_i = \omega_i t. \quad (16)$$

Under constant speed, the stator of the synchronous motor can be modeled by a per-phase equivalent circuit consisting of a resistance R_i , an inductance L_i and a back electromotive force (EMF) V_i at the frequency ω_i . When the motor is fed by the PWM inverter of Fig. 1, the power balance equation of (8) can be rewritten as

$$i_2 V_c = 3V_i I_i \cos \phi_i + 3R_i I_i^2 + 3I_i L_i \frac{dI_i}{dt}. \quad (17)$$

The phase current I_i is controlled by I_{mag} . The voltage magnitude V_i is controllable by the field current of the synchronous motor. For a fixed field current, V_i increases linearly with ω_i . The phase angle ϕ_i can be changed by

resetting the position encoder mounting or by readdressing the EPROM.

One condition to be noted is in the last term of (17). Since it involves a differentiation, it is obvious that I_i should not change instantaneously. A step change theoretically implies an impulse on differentiation. Physically it means that the inductive storage energy should not be changed abruptly. For this reason, the test function will consist of ramps in this study.

Regulated Rectifier

On an ac power supply side, one can model a regulated rectifier as a per-phase equivalent circuit consisting of a resistance R_r , an inductance L_r , and an ideal voltage V_r . The power balance (6) becomes

$$i_1 V_c = 3V_r I_r \cos \phi_r - 3R_r I_r^2 - 3I_r L_r \frac{dI_r}{dt}. \quad (18)$$

Using a proportional feedback, the rectifier current is

$$I_r = K_1 (V_{co} - V_c) \quad (19)$$

where K_1 is the transfer gain and V_{co} is the open circuit voltage.

Substituting (19) into (18) and i_1 into Kirchoff's current law at the node of the capacitance

$$C \frac{dV_c}{dt} = i_1 - i_2, \quad (20)$$

one has

$$\frac{dV_c}{dt} = \frac{3K_1 [V_c \cos \phi_r (V_{co} - V_c) - K_1 R_r (V_{co} - V_c)^2] - i_2 V_c}{[C V_c - 3K_1^2 L_r (V_{co} - V_c)]} \quad (21)$$

SIMULATION STUDY

Fig. 10 shows the digital simulations based on solving (17) and (21) simultaneously. It is assumed that the motor is turning at a constant speed. The parameters in the study are: $V_i = 30$ V, $\cos \phi_i = 1$, $R_i = 0.2$ ohm, $L_i = 0.013$ H, $V_r = 30$ V, $R_r = 0.2$ ohm, $L_r = 0.013$ H, $V_{co} = 110$ Vdc, $K_1 = 3.21$ A/V, $\omega_i = 377$ rad/s, $\cos \phi_r = 1$, $C = 24\,000$ μ F.

The command is inputted as I_{mag} and I_i is proportional to it. The test function of the inverter current I_{mag} is in the form of a succession of ramp and constant values as shown in Fig. 10(a). The initial condition is at $t = 0$, $V_c = V_{co} = 110$ Vdc.

The current i_2 is solved from (17), given I_i and V_c at successive instants of time. The presence of the dI_i/dt term is evident in Fig. 10(d), which shows i_2 being shifted up and down because of the step function introduced by the differentiation of the ramp.

In Fig. 10(b) one sees that under motoring conditions V_c is below $V_{co} = 110$ V and, conversely, above V_{co} when the motor is braked. It is the polarity of the error which commands the direction of power flow in the rectifier. The capacitance current i_{CAP} in Fig. 10(c) comes from the difference between i_1 and i_2 in Fig. 10(d). It is the charg-

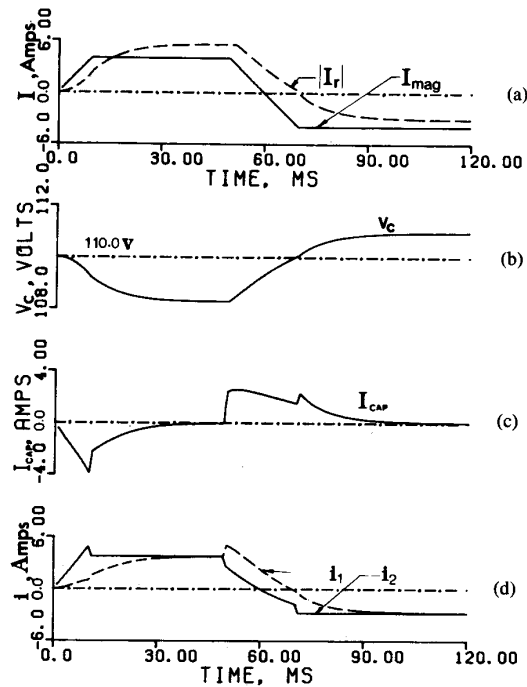


Fig. 10. Digital simulation of synchronous motor drive. (a) AC current of rectifier tracking inverter current command. (b) DC link voltage. (c) Capacitor charging current. (d) DC link rectifier and inverter current (local averages).

ing or the discharging of the capacitance by i_{CAP} which causes V_c to increase or decrease.

It should be noted from Figs. 6 and 7 that the dc link current actually consists of a sequence of switching pulses. As such, i_1 and i_2 , which are solved from the power balance equations (18) and (17), are the local average values of the switching pulses.

CONCLUSION

An integrated controlled-current PWM rectifier/inverter link has been implemented and tested with a polyphase induction motor. The design takes into account the special peculiarities of the controlled-current PWM modulator, viz., 1) the loss of control limit and 2) the current waveform distortion limit must be respected; and 3) the modulators are current-controlled devices. Bidirectional current flow in the dc link is achieved without bidirectional power switches.

ACKNOWLEDGMENT

The authors are grateful to Professor H. C. Lee for the loan of certain laboratory equipment, Mr. J. Mui for laboratory assistance, and Mrs. P. Menon for the preparation of the manuscript. Mr. J. W. Dixon thanks the Catholic University of Chile for financial assistance in his post-graduate studies.

REFERENCES

- [1] T. Kataoka, K. Mizumachi, and S. Miyairi, "A pulsewidth controlled ac-to-dc converter to improve power factor and waveform of ac line

current," *IEEE Trans. Ind. Appl.*, vol. IA-15, pp. 670-675, Nov./Dec. 1979.

- [2] D. Carroll, S. S. Abdel-Hamid, and F. Nozari, "A simplified analytical model for a current-fed force commutated converter," *IEEE Trans. Ind. Appl.*, vol. IA-16, pp. 501-512, July/Aug. 1980.
- [3] H. Zander, "Self-commutated rectifier to improve line conditions," in *Proc. IEEE*, vol. 120, No. 9, Sept. 1973.
- [4] N. Matsui and Y. Ohashi, "A microcomputer-based commutation failure free control system for the cascaded rectifier circuit," *IEEE Trans. Ind. Elect. Cont. Instr.*, vol. IECI-28, pp. 380-387, Nov. 1981.
- [5] Kocher and Steigerwald, "An ac-to-dc converter with high quality input waveforms," *IEEE Trans. Ind. Appl.*, vol. IA-19, No. 3, July/Aug. 1983, pp. 586-599.
- [6] B. T. Ooi, J. C. Salmon, J. W. Dixon, and A. B. Kulkarni, "A 3-phase controlled current PWM converter with leading power factor," *IEEE-IAS Annual Meeting*, Toronto, pp. 1008-1014, Oct. 1985.
- [7] E. P. Weichmann, P. D. Ziogas, and V. R. Stefanovic, "A novel bilateral power conversion scheme for variable frequency static power supplies," *IEEE Trans. Ind. Appl.*, vol. IA-21, pp. 1225-1233, Sept./Oct. 1985.
- [8] P. D. Ziogas, Y. G. Kang, and V. R. Stefanovic, "PWM control techniques for rectifier filter minimization," *IEEE Trans. Ind. Appl.*, vol. IA-21, pp. 1206-1213, Sept./Oct. 1985.
- [9] H. Kohlmeier, O. Niermeger, and D. Schroder, "High dynamic four quadrant ac-motor drive with improved factor on-line optimized pulse pattern with PROMC," *IEEE-IAS Annual Meeting*, Toronto, pp. 1081-1086, October 1985.
- [10] M. Lajoie-Mazenc, C. Villamieva, and J. Hector, "Study and implementation of hysteresis controlled inverter on a permanent magnet synchronous motor," *Conf. Rec., IEEE-IAS 1984 Annual Meeting*, pp. 426-431, 84CH2060-2.



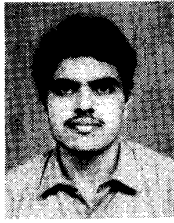
Boon Teck Ooi (S'69-M'71-SM'85) received the B.Eng. Hons. degree from the University of Adelaide, Australia, the S.M. degree from the Massachusetts Institute of Technology, Cambridge, and the Ph.D. degree from McGill University, Montreal, PQ, Canada.

His research interests have included linear induction motors, electrodynamic magnetic levitation with superconducting magnets, subsynchronous resonance phenomena, stability of long-distance power transmission, HV dc, and power electronics. He is presently a Professor in the Department of Electrical Engineering at McGill University.



Juan W. Dixon was born in Santiago, Chile. He received the Electrical Engineering degree from the University of Chile in 1977. In 1986 he received the M.Eng. degree in electrical engineering from McGill University, Montreal, PQ, Canada, where he is presently working towards the Ph.D. degree in electrical engineering.

From 1977 to 1979 he worked for Ferrocarriles del Estado, the Chilean national railways company, as a Chief of the Electrical Locomotives Section. Since May 1979 he has been working at the Catholic University of Chile as a Professor in Electrical Machines and Power Electronics.



Ashok B. Kulkarni was born in Bangalore, India. He obtained the B.E. degree from Bangalore University, Bangalore, India, in 1981 and the M. Tech degree from the Indian Institute of Technology, Madras, in 1983, both in electrical engineering. He received the M.Eng. degree in electrical engineering from McGill University, Montreal, PQ, Canada, in 1986. He is presently a Ph.D. candidate at Texas A&M University, College Station.

He worked with M/S Tata Consulting Engineers, Bangalore, during 1983-1984 as a Postgraduate Engineer.



Masahiro Nishimoto was born in Japan. He obtained the B.Eng. degree from Hiroshima Institute of Technology, Hiroshima, Japan, and the M.Eng. degree from McGill University, Montreal, PQ, Canada, both in electrical engineering. He is currently a Ph.D. candidate at McGill University.

From 1971 to 1983 he worked as a design engineer of control systems of steam power plants and held the position of Power Plant Manager.